AFRL-AFOSR-JP-TR-2017-0004

Micro and nanostructured materials for fluid and ion transport for miniaturized applications

Paulo Lozano
MASSACHUSETTS INSTITUTE OF TECHNOLOGY

06/08/2016
Final Report

Air Force Research Laboratory
AF Office Of Scientific Research (AFOSR)/ IOA
Arlington, Virginia 22203
Air Force Materiel Command

REPORT DOCUMENTATION PAGE

Form Approved
OMB No. 0704-0188

1. REPORT DATE *(DD-MM-YYYY)*	**2. REPORT TYPE**	**3. DATES COVERED** *(From - To)*
18-01-2017	Final	09 Sep 2014 to 08 Mar 2016

4. TITLE AND SUBTITLE
Micro and nanostructured materials for fluid and ion transport for miniaturized applications

5a. CONTRACT NUMBER

5b. GRANT NUMBER
FA2386-14-1-4067

5c. PROGRAM ELEMENT NUMBER
61102F

6. AUTHOR(S)
Paulo Lozano

5d. PROJECT NUMBER

5e. TASK NUMBER

5f. WORK UNIT NUMBER

7. PERFORMING ORGANIZATION NAME(S) AND ADDRESS(ES)
MASSACHUSETTS INSTITUTE OF TECHNOLOGY
77 MASSACHUSETTS AVE
CAMBRIDGE, MA 02139-4301 US

8. PERFORMING ORGANIZATION REPORT NUMBER

9. SPONSORING/MONITORING AGENCY NAME(S) AND ADDRESS(ES)
AOARD
UNIT 45002
APO AP 96338-5002

10. SPONSOR/MONITOR'S ACRONYM(S)
AFRL/AFOSR IOA

11. SPONSOR/MONITOR'S REPORT NUMBER(S)
AFRL-AFOSR-JP-TR-2017-0004

12. DISTRIBUTION/AVAILABILITY STATEMENT
A DISTRIBUTION UNLIMITED: PB Public Release

13. SUPPLEMENTARY NOTES

14. ABSTRACT
Ionic Liquid Ion Sources (ILIS) are devices capable of producing molecular ion beams through electrostatic stressing of room temperature molten salts, or ionic liquids. These ion beams can be applied in space propulsion, in focused ion beams for microfabrication and in reactive ion etching. To achieve ion evaporation from the ionic liquid, the liquid is supported on a micron-sized emitter tip. The emitter is subjected to an electric field to deform the liquid into a sharp meniscus, at the apex of which the electric field can be high enough to trigger ion evaporation. Novel emitter configurations are required to guarantee the stable operation of these sources in the pure ion regime (PIR) with no intervening droplets. With AOARD support, analytical estimates have been performed to determine tip geometries and substrates morphologies required for the emitter to support PIR operation. Furthermore, novel nanomaterials have been investigated as alternative ILIS substrates. In particular, porous carbon xerogels have been identified as emitter materials, as they have outstanding pore uniformity, are easy to shape into the required geometries, and are compatible with ionic liquids. These substrates also have the adequate pore sizes and porosities established by the analytical estimates.

15. SUBJECT TERMS
ionic liquids, fluid and ion transport

16. SECURITY CLASSIFICATION OF:			**17. LIMITATION OF ABSTRACT**	**18. NUMBER OF PAGES**	**19a. NAME OF RESPONSIBLE PERSON**
a. REPORT	**b. ABSTRACT**	**c. THIS PAGE**			CASTER, KENNETH
Unclassified	Unclassified	Unclassified	SAR	12	**19b. TELEPHONE NUMBER** *(Include area code)* 315-229-3326

Standard Form 298 (Rev. 8/98)
Prescribed by ANSI Std. Z39.18

Final Report for AOARD Grant FA2386-14-1-4067

"**Micro- and nanostructured materials for fluid and ion transport for miniaturized applications**"

Date 6/6/16

Name of Principal Investigators:

- e-mail address : plozano@mit.edu
- Institution: Massachusetts Institute of Technology
- Mailing Address: 77 Massachusetts Ave 37-401, Cambridge, MA 02139 USA
- Phone: (617) 258-0742
- Fax : none

Co-PI: Li-Chyong Chen

- e-mail address: chenlc@ntu.edu.tw
- Institution: National Taiwan University
- Mailing Address: 1 Roosevelt Road, Section 4, National Taiwan University, Taipei, Taiwan
- Phone: 886-2-3366-5249

Period of Performance: 9/9/14-3/8/16

Abstract:

Ionic Liquid Ion Sources (ILIS) are devices capable of producing molecular ion beams through electrostatic stressing of room temperature molten salts, or ionic liquids. These ion beams can be applied in space propulsion, in focused ion beams for microfabrication and in reactive ion etching. To achieve ion evaporation from the ionic liquid, the liquid is supported on a micron-sized emitter tip. The emitter is subjected to an electric field to deform the liquid into a sharp meniscus, at the apex of which the electric field can be high enough to trigger ion evaporation. Novel emitter configurations are required to guarantee the stable operation of these sources in the pure ion regime (PIR) with no intervening droplets. With AOARD support, analytical estimates have been performed to determine tip geometries and substrates morphologies required for the emitter to support PIR operation. Furthermore, novel nanomaterials have been investigated as alternative ILIS substrates. In particular, porous carbon xerogels have been identified as emitter materials, as they have outstanding pore uniformity, are easy to shape into the required geometries, and are compatible with ionic liquids. These substrates also have the adequate pore sizes and porosities established by the analytical estimates. Carbon xerogel emitters have been produced through mechanical polishing, and stable emission has been obtained with the ionic liquid 1-ethyl-3-methylimidazolium tetrafluoroborate. Time-of-flight (TOF) spectrometry has been used to verify that the mechanically polished source operates in the pure ionic regime. Given the encouraging results with the mechanically polished emitter, more repeatable manufacturing techniques have been researched. Laser micromachining can be used to shape the carbon xerogel into emitters. TOF spectrometry and retarding potential energy analysis indicate the operation of the laser micromachined tip in the PIR. AOARD funding has allowed our team to support students at the undergraduate and graduate levels. It has also lead to publications in refereed journals and the creation of intellectual property. Some results from the fundamental research generated in this work have transitioned into development programs in other DoD agencies.

Introduction:

Ionic Liquid Ion Sources (ILIS) produce ion beams through field evaporation from room temperature molten salts, or ionic liquids [1]. These ion beams can be used for applications in nanofabrication, such as reactive ion etching [2] and focused ion beams [3], as well as in space propulsion [4]. Ion extraction is obtained by stressing the ionic liquid into a sharp meniscus, formed on the apex of micro-sized, nanostructured tips known as emitters. The goal of this

research is to design, construct and test novel emitter configurations for the transport of ionic liquids to the electrified meniscus.

ILIS technology requires highly stable, repeatable and predictable operation in the pure ionic regime (PIR), which has been elusive in previous implementations. Operation of the electrospray from an ionic liquid in the PIR is controlled by the liquid's physical properties, in particular the conductivity K and by the flow rate Q provided by the emitter. The electric field on the ion meniscus scales [5] as $E \sim (K/Q)^{1/6}$, and thus the emitter must have a sufficiently high hydraulic impedance to reduce the flow rate and guarantee that the electric field will reach the value required for field-evaporation from the ionic liquid. Pure ion emission was first demonstrated from actively fed capillaries using the liquid 1-ethyl-3-methylimidazolium tetrafluoroborate (EMI-BF_4) [6]. It is possible to achieve the PIR from capillaries operating close to the minimum flow rate under which the electrostatic balance is sustainable and liquid conductivity greater than 1 S/m and large surface tension [7]. However, operation in the mixed regime is more common with this configuration due to the larger flow rates supported by a capillary. Pure ion emission can be readily achieved from externally wetted emitters for a number of ionic liquids thanks to the high hydraulic impedance of this configuration [8,9]. Nonetheless, the surface treatments required to achieve wetting of the surface often create uneven features near the emitter apex, which promote menisci anchoring away from the apex itself. This off-axis emission is not acceptable for focusing applications and might lead to extractor electrode degradation. Pure ion emission has also been achieved from porous tungsten emitters [10]. However, most porous metals are usually sintered from relatively large and polydisperse powder populations, making it difficult to shape such metals into sharp structures with repeatability. Furthermore, poor wetting of the ionic liquid on metals leads to off-axis emission from individual pores rather than from a single meniscus on the tip apex [11]. Therefore, there is a need for new emitter structures that provide a continuous supply of liquid compatible with the ion evaporation process, and that have a geometry that favors the formation of the electrified meniscus in the correct tip location to prevent instabilities.

During the first year of the reporting period, we made key advances into finding new emitter configurations with adequate transport properties for PIR operation. Analytical estimates have been used to estimate target tip sharpness and porous substrate properties that restrict the flow rate. Porous carbon xerogel substrates can be synthesized with the required pore sizes and porosities [12,13], and what is more, these materials have outstanding pore uniformity, are easy to machine by additive and subtractive processes, and have the advantage that carbon is well wetted by ionic liquids [14]. Carbon xerogel has been mechanically polished into microtips with the adequate geometry from the analytical estimates. Stable operation of the mechanically polished tip in the PIR has been confirmed using time-of-flight (TOF) spectrometry. These high impact results have been published in Applied Physics Letters [15]. Over the last months of the reporting period, the implementation of the carbon xerogel emitter has been revisited. Laser micromachining has been used to fabricate emitter structures with higher reliability. The laser micromachined tip has been implemented with an integrated liquid reservoir, and TOF and retarding potential analysis (RPA) experiments indicate the operation of this improved configuration in the PIR.

Design and experiment with mechanically polished carbon xerogel tips

Analytical estimates have been used to determine the required substrate morphologies and tip dimensions in order to ensure that the emission from the tip will be purely ionic. The emitter's hydraulic impedance should exceed $Z_{min} = 1.5 \times 10^{17}$ $kgs^{-1}m^{-4}$, which is the lowest impedance reported for which the PIR has been achieved with the ionic liquid EMI-BF_4 [16,17]. The hydraulic impedance of a porous conical structure can be derived [18] as a function of its height h, half-angle α, tip radius of curvature R_c, and substrate permeability κ and is given by

$$Z = \frac{\mu}{2\pi\kappa} \frac{1}{1-\cos\alpha} \left(\frac{\tan\alpha}{R_c} - \frac{\cos\alpha}{h} \right) \quad [1]$$

Where μ is the viscosity of the ionic liquid (0.038 Pa s for EMI-BF_4 [19]). For high aspect ratio emitters ($h/R_c > 10$), the impedance is governed by the first term of equation (1). Typical emitters used with ionic liquids have radii of curvature ranging between a few and tens of microns. For $R_c = 5$ μm and $\alpha = 20°$, κ should be maintained below 10^{-13} m^2 to exceed the baseline impedance. The substrate permeability can be computed as a function of the pore radius and porosity [18]. For typical porosities between 0.4 and 0.6, the substrate should have pore radii below 1 μm to guarantee low enough permeability and achieve the target emitter impedance. Therefore, the tip design goal is a half angle of about $20°$, radius of curvature on the order of 5 μm, and pore radii of 1 μm or less.

Test emitters are fabricated by mechanical polishing of the carbon xerogels, synthesized in-house. The starting material is resorcinol-formaldehyde xerogel synthesized using modified procedures from Reference [20], as described by Reference [21]. The starting sol consists of 24.6 g of resorcinol (Sigma Aldrich) dissolved in 30 g of water and 35.8 g of formaldehyde solution 37 % solution in water (Sigma-Aldrich). The crosslinking between the resorcinol and formaldehyde is catalyzed using 0.88 g of acetic acid (Sigma-Aldrich). The mixture is then poured into molds, sealed, and allowed to gel in a carefully controlled thermal cycle. The molds are then opened to evaporate the solvent from the gel structure and obtain a solid polymer.

To fabricate a microtip, a cylinder of the resorcinol formaldehyde xerogel is mechanically polished to a conical shape. The cone structure is subsequently pyrolized at 900 °C for 3 h under an argon atmosphere. The resulting material is a carbon porous network with pore diameters slightly below 1 μm, as estimated from SEM images. For a porosity of 0.6 [21], the permeability is $\kappa = 3\times10^{-14}$ m^2. At this point, the samples are polished again to remove some foreign contamination and refine the emitter apex, and the formed tips are then cleaned in ultrasonic baths of acetone and isopropanol. SEM images of the apex of a sample test emitter are shown in Figure 1(a) and 1(b). The resulting half-angle is closer to 25° due to fabrication variations, and the estimated tip curvature is about 7 μm. With these values, the estimated impedance of the resulting emitters is about twice Z_{min}.

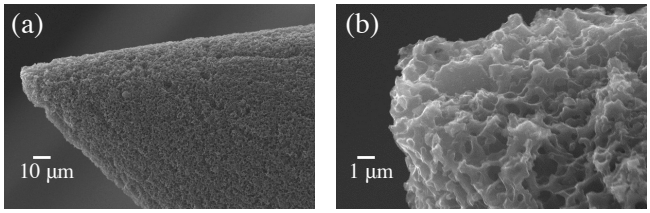

Figure 1. Scanning Electron Micrographs of Carbon Xerogel Test Emitter.

The emitter is prepared for emission by installing a distal electrode contact [22]. The electrical contact is a platinum wire, wrapped around the emitter, and electrically isolated from it using fiberglass. The emitter, fiberglass, and distal contact are then immersed in a crucible of EMI-BF_4 under vacuum conditions (to eliminate water and residual gases from the porous structure [23]) before being installed in the setup for emission and TOF experiments.

Figure 3 shows the experimental setup. The emitter is centered in front of a metallic aperture (the extractor), which is followed by another plate that acts as a shield. The shield supports a small magnet that helps to eliminate spurious signals from secondary electron emission resulting from ion beam impingement on the setup surfaces. The voltage applied to the distal electrode, V_{app}, is provided by a high voltage bipolar power supply, and the current emitted by the source, $I_{emitted}$, is measured by reading the voltage drop across a resistor connected in series with the power supply. The TOF setup consists of a set of deflector plates, an electrostatic deflection gate, and a channeltron detector. To determine the composition of the emission, the gate periodically deflects the beam away from the channeltron. By measuring the time-of-flight t of the beam particles across the known distance L (set to 0.75 m), it is possible to find their charge-to-mass ratio q/m,

assuming that their energy is equal to the applied voltage, from the following relationship:

$$t = L\sqrt{\frac{m}{2qV_{app}}} \quad (2)$$

The deflector plates consist of two pairs of parallel planar electrodes, which can be used to stir the beam by biasing the plates to a few tens of volts. The gate consists of several grounded apertures enclosing two electrodes of length 6.25 mm along the path of the beam, biased to +/-950 V, operated at a frequency of 500 Hz. All experiments are performed at pressures below 10^{-3} P and at 29 °C.

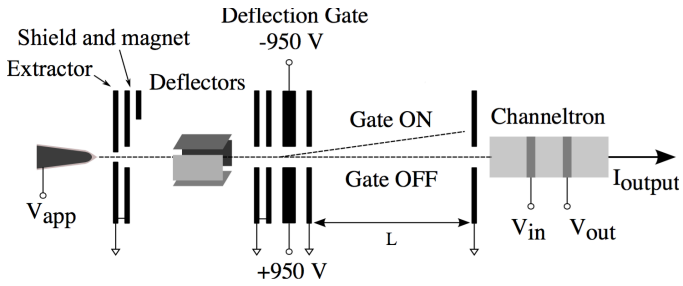

Figure 2. Experimental setup for emission and TOF experiments.

Results: mechanically polished carbon xerogel emitter

Stable emission is obtained from the carbon xerogel microtip. Triangular voltage signals and alternating voltage ramps are applied to the distal contact to determine the source response. Figures 3(a) and (b) show a sample voltage signal and the corresponding emitted current. Emission occurs at a threshold voltage of +/-1535 V for this particular implementation and the current levels are of the order of a few hundred nA, which is similar to the response from externally wetted emitters [24]. Figure 3(c) shows the average current for each of the voltages tested in the stepped ramp from Figures 3(a) and 3(b). Three emission regimes can be identified. First, the source emits intermittently at voltages close to the startup potential, as the electrostatic traction is insufficient for sustaining continuous emission. When V_{app} is increased, the source emission becomes uninterrupted, showing an overshoot as the voltage is switched and reaching a stable current within a few seconds. When V_{app} is increased over a certain value, the current shows a clear step, which is consistent with the appearance of a second emission site supported farther upstream on the emitter apex. The source displays excellent short-term stability in the intermediate voltage range. Figure 3(d) shows 2-min intervals of operation of the source in the positive and negative polarity. The variation of the current (standard deviation/mean) is less than 1%, suggesting an adequate liquid supply to the emission site.

TOF spectrometry reveals that the emitter operates in the PIR with the ionic liquid EMI-BF_4. The deflector plates are biased to direct the beam towards the detector and perform a coarse scan in several directions, thus obtaining TOF data from several locations over the cross-section of the beam. Figure 4 shows sample TOF traces obtained with the source operating at V_{app} =1818 V. The relative intensities of the four signals are illustrated in the inset. Each current signal has been normalized to its own maximum for clarity, and the time-of-flight axis has been coverted to mass units making use of equation (2) and assuming singly charged species. The current steps correspond closely to the mass of the ions EMI^+, (EMI-BF_4)EMI^+ and (EMI-BF_4)EMI^+ (111, 309, and 507 amu, respectively). The signal slopes between the steps and before the current reaches its maximum value correspond to the results of the fragmentation of heavy ions (EMI-BF_4)$_n$$EMI^+$ (n=1,2,3, …) into neutrals and lighter ions, which have a fraction of their original kinetic energy. TOF traces on different beam sections and from experiments at different operating voltages show the same behavior and no droplet signals.

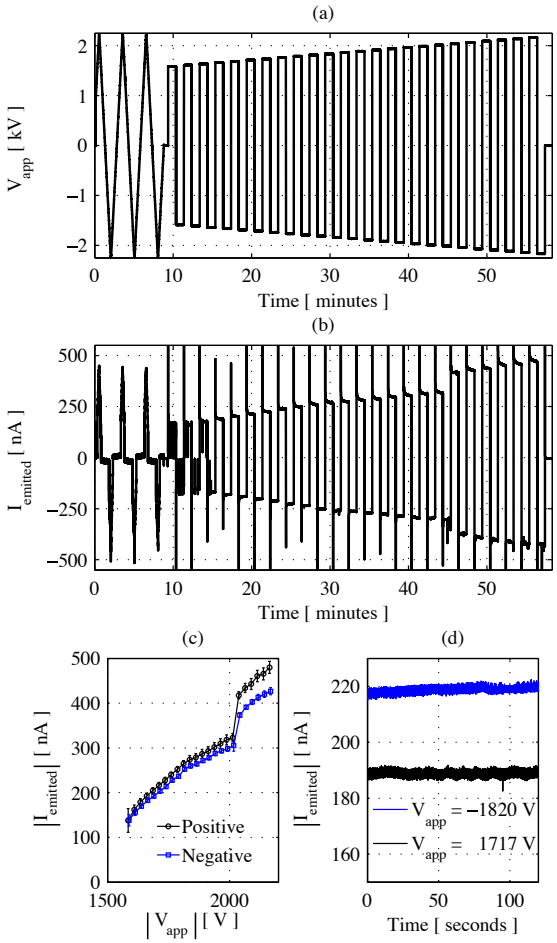

Figure 3. Current-voltage response of the mechanically polished carbon xerogel ILIS emitter.

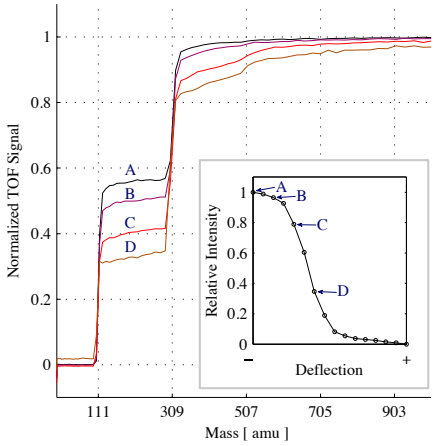

Figure 4. Time-of-flight profiles for different locations over the cross section of the beam; inset shows the beam current profile along a particular linear scan. Curve A corresponds to the TOF signal of maximum intensity in the scan.

The tests with the carbon xerogel emitter demonstrate that this substrate has adequate transport properties to facilitate operation in the pure ionic regime. Therefore, carbon xerogel emitters could be used to study the performance of ILIS in the proposed applications. The mechanical polishing technique used for the creation of the prototype carbon emitter has a low yield and poor repeatability. As a result, laser micromachining has been introduced as a manufacturing technique for the shaping of carbon xerogel tips. This fabrication method should allow the repeatable fabrication of the carbon xerogel into single emitters or tip arrays. Besides the change in fabrication technique, the implementation of the carbon emitter has been revisited, and the source is now implemented with an integrated reservoir. The new design, manufacturing process and characterization results are discussed next.

Laser micromachined carbon xerogel emitters

For optimal long-term operation, the carbon xerogel ILIS should be in contact with a reservoir that replenishes the ionic liquid consumed by the tip. The carbon xerogel ILIS is implemented in a cylindrical teflon container with an integrated reservoir, as shown in Figure 5(a). The teflon piece has a cavity that fits the cylindrical piece of carbon xerogel with the carbon tip, as well as another cavity that contains the distal contact (a Pt wire) and acts as a reservoir. In order to isolate electrically the distal contact from the carbon piece containing the tip, a piece of fiberglass is used as a spacer. The fiberglass also provides wicking form the reservoir to the porous carbon structure.

Laser ablation has been used to shape single emitters on carbon xerogel monoliths. The laser facility in the Space Propulsion Laboratory consist of a KrF excimer laser (248 nm wavelength), a set of optics to shape, direct and focus the beam, and a micropositiong stage for movement of the sample. The laser produces 17 ns pulses of 200 mJ energy at a frequency of 200 Hz. The optics focus the beam into a spot approximately 53 μm in diameter. The carbon xerogel monolith is rastered beneath the fixed laser spot in order to ablate material and create the emitter structure. The stage movement process has been optimized to produce 300 μm tall tips with radii of curvature between 5 and 10 μm, as shown in Figures 5(b)-(e).

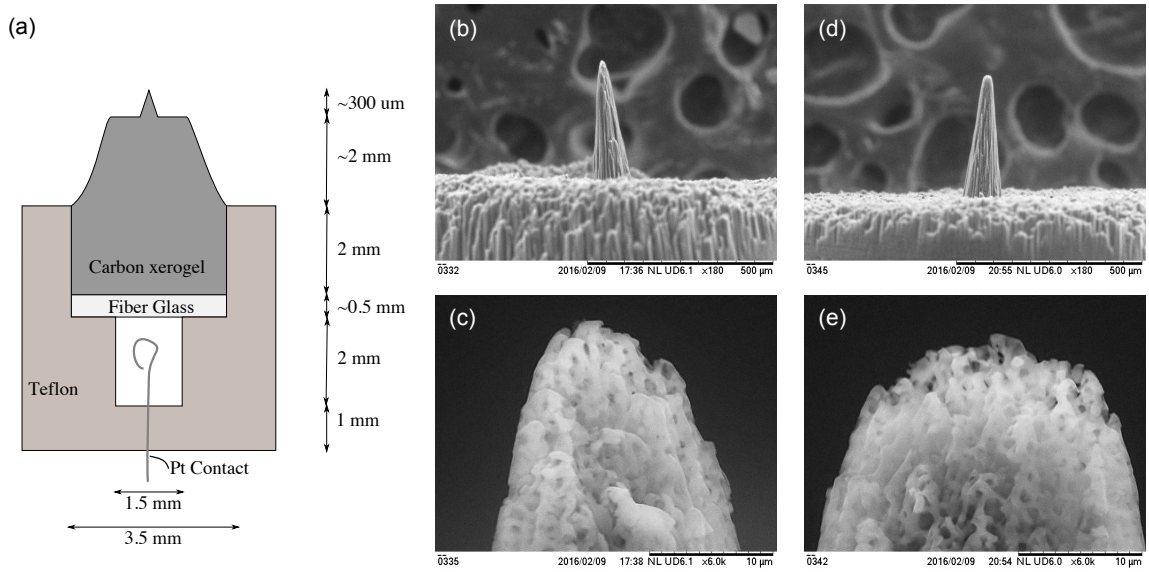

Figure 5. (a) Revised emitter implementation geometry (b)-(e) SEM images of laser micromachined tips, images (b) and (c) correspond to one emitter, (d) and (e) to another.

The laser micromachined tip shown in Figures 5(d),(e) is mounted on the teflon cylinder which has been prefilled with the ionic liquid EMI-BF_4. The emitter assembly is then placed in the same characterization setup used for the mechanically polished tip (see Figure 2). Note that for these

tests, the TOF setup does not have the deflection plates before the gate, and so the TOF profiles correspond solely to the beam section that is aligned with the channeltron detector.

The emitter's current-voltage (IV) relationship and TOF profiles were obtained. The IV relation is shown in Figure 6(a). The source has a startup voltage of approximately ± 1720 V, and the emission is intermittent at voltages close to the start-up voltage. As the magnitude of the voltage is increased, the emission becomes stable. Current levels of 300 nA are observed once the source is stable, which are consistent with operation from a single emission site. As the voltage is increased, the current can by increased up to 550 nA before a discontinuity in the current is observed. This discontinuity is likely caused by the appearance of a second emission site. On the ramp down, this second emission site displays an extinction voltage lower than its onset voltage. On the negative ramp, a similar behavior is observed. The higher currents observed with the laser micromachined tip as compared to the mechanically polished tip might be attributed to a larger R_c.

The TOF results indicate operation in the pure ion regime. For these experiments, the gate was turned on at t=0 μs, and so the channeltron displays current drops as the different particles stop arriving. Figure 6(b) shows the normalized TOF signals obtained at different operating voltages, with the x-axis showing the mass in atomic units obtained from the flight time and equation (2). There are clear steps in the signal at 111 and 309 amu, which correspond to the monomer and dimer ions in the beam. The signal drops from 4% to the noise level between 507 amu (corresponding to n=3) to 1685 amu (n=9), indicating that there are some heavier cluster ions in the emitted beam.

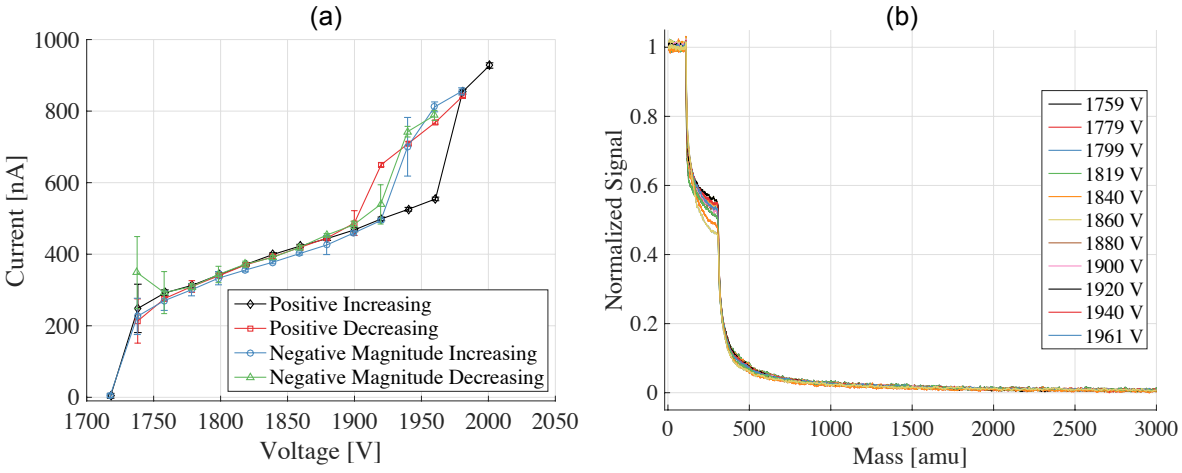

Figure 6. (a) IV response and (b) TOF profiles at different V_{app} (indicated in the legend) of the laser micromachined carbon xerogel tip.

To complement the TOF measurements, RPA experiments have been performed with the laser micromachined tip. The setup is shown in Figure 7(a). The RPA instrument consists of a Faraday cup collector and a set of grids placed in between the emitter and the collector. If the bias of the retarding grids, V_{RP}, exceeds the energy of the particle in the beam, the particle cannot reach the collector. Therefore, by varying the retarding potential and measuring the current arriving to the Faraday cup, it is possible to obtain the beam energy distribution.

The instrument consists of seven grids followed by a Faraday cup. The first grid is a 90% transparent tungsten mesh, which is grounded and located approximately 25 mm downstream from the extractor. The next five grids are the retarding grids, with a 90% transparency for each grid. The last grid before the Faraday cup is a tungsten mesh biased to a potential V_{SE}, set in these experiments to -25 V. This last grid suppresses spurious current signals due to secondary

electron emission from the Faraday cup. The Faraday cup is connected to a current amplifier whose signal is recorded in an oscilloscope.

To perform RPA experiments, the source is held at a constant voltage, and a high voltage triangular wave, varying between 0 and a voltage of slightly greater magnitude than V_{app}, is applied to the retarding grids, at a period of 10 s. The current signal from the Faraday cup is processed using a low pass filter and a sorting algorithm. The signals are then normalized to the maximum signal detected in the collector. The results from the experiments at different operation voltages of the source are shown in Figure 7(b).

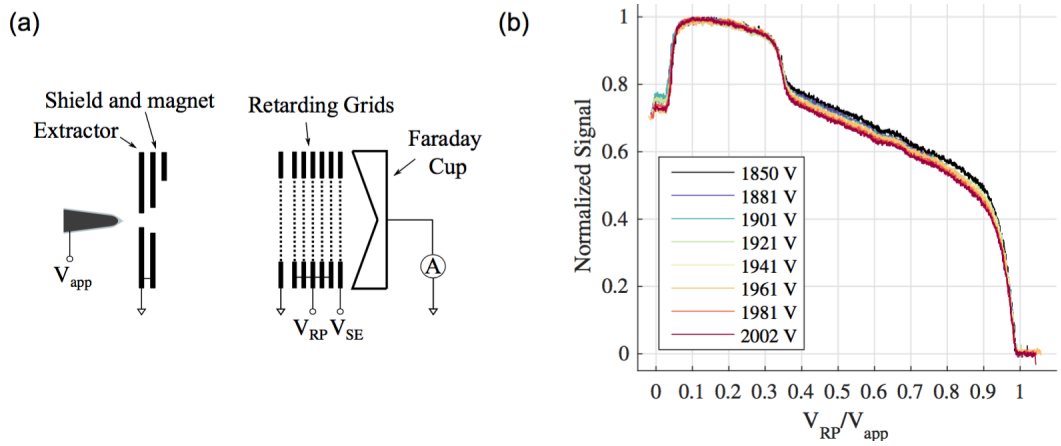

Figure 7. (a) RPA Setup (b) RPA signals at different operation voltages (indicated in the legend) of the laser micromachined tip.

The results from Figure 7(b) are a coarse profile of the beam energy distribution, as there are several artifacts that can be attributed to the instrument. First, for retarding potentials of about $0.05V_{app}$, an increase in the current collected is detected, probably due to a focusing effect from the retarding grids. Furthermore, the instrument introduces an artificial spread in the energies detected due to geometrical effects. An ion with energy qV_0 should ideally be stopped by a potential barrier $V_{RP}=V_0$. However, an ion of energy V_0 coming at an angle θ with respect to the optical axis will be deflected by a potential $V_{RP}=V_0 cos^2\theta$. Since the RPA instrument is capturing the whole beam, the current drops corresponding to monochromatic ion populations will have an artificial spreading. For instance, in Figure 7(b), there is a current drop close to the applied potential that likely corresponds to the ions that have been fully accelerated to within 10 V of the acceleration potential, as observed in previous ILIS [26]; however, this drop occurs over a range of several tens of volts that is greater than the spreads that are expected from ILIS.

Taking into account these artifacts, it is possible to discern some of the physics of the ion beam from the RPA data. About half of the beam corresponds to ions coming close to the full acceleration potential. The data also shows the occurrence of fragmentation of solvated ions in the beam. These fragmentation events have been observed in previous ILIS [26]. The energy of a fragmented ion is a fraction of the kinetic energy of the parent ion, with an extra contribution if the break-up occurred in a region of non-zero potential. If an ion with degree of solvation n and mass m_n breaks into a neutral and an ion with degree of solvation m (m < n) and mass m_m, at a region with potential V_b (such as the region between the emitter and the extractor, where the potential varies from V_{app} to ground), the final kinetic energy of the ion resulting from breakup will be

$$K_m = q\frac{m_m}{m_n}\left|V_{app} - V_b\right| + qV_b \quad (3)$$

Thus, a fragmented ion will be stopped at a potential $V_{RP}=K_m/q$. In the figure, a distinct current drops can be observed at $V_{RP} \approx 0.36V_{app}$. This retarding potential corresponds to the fragmentation of dimers into monomers after the beam has been fully accelerated, as indicated

by equation 3 (the ratio of masses is 111/309). There is a continuous current drop between the retarding potential for the 2 → 1 fragment ions and the main current drop, which indicates that fragmentation is occurring in between the emitter and the extractor. The RPA signals show a particle population coming at low energies, between $0.1V_{app}$ and $0.36V_{app}$. These signals may be caused by fragmentation of cluster ions (with 4-9 neutrals attached) into monomers. This would be consistent with the TOF results that show a small component of cluster ions in the beam.

Summary and Project Impact

The AOARD grant has allowed the demonstration of carbon xerogel as a suitable emitter material for ionic liquid ion sources. TOF experiments with mechanically polished prototype emitters demonstrate that the material has adequate liquid transport properties to operate in the purely ionic regime ideal for the intended applications. Laser micromachining has been validated as a manufacturing technique for shaping the carbon xerogel substrate into emitter tips. This technique should be useful for the repeatable fabrication of single emitter tips for FIB or for the patterning of tip arrays for propulsion or etching applications. The laser micromachined tip operates in the purely ionic mode as demonstrated by TOF and RPA analysis. The results of this research have allowed a number of transitions within the US Government and industry. All of the IP generated has been licensed to an MIT spinoff named Accion Systems, that aims to commercialize electrospray thrusters for different commercial and government customers. In addition, the research has lead to different research programs, in particular with the development of specialized materials and techniques for micropropulsion for AFOSR (study on fluoro-hydrogenated ionic liquids) and the US Government for the demonstration of electrospray propulsion in space.

List of Publications that result form your AOARD supported project

[1] C. Perez-Martinez and P.C. Lozano, Ion field-evaporation from ionic liquids infusing carbon xerogel microtips, Applied Physics Letters, 107, 043501 (2015)
[2] C. Perez-Martinez, Ph.D. Thesis, Dept. of Aeronautics and Astronautics, Massachusetts Institute of Technology, Cambridge MA (May 2016)

References

[1] P. Lozano and M. Martinez-Sanchez, J. Colloid Interface Sci. 282, 415 (2005)
[2] C. Perez-Martinez *et al.*, J. Vac. Sci. Technol. B 28, L25 (2010)
[3] A.N. Zorzos and P.C. Lozano, J. Vac. Sci. Technol. B 26, 2097 (2008)
[4] P. Lozano, M. Martinez-Sanchez, and V. Hruby, in *Encyclopedia of Aerospace Engineering: Electrospray Propulsion* (John Wiley and Sons, 2010)
[5] M. Gamero-Castano and J. Fernandez de la Mora, J. Chem. Phys. 113, 815 (2000)
[6] I. Romero-Sanz, R. Bocanegra, J. Fernandez de la Mora, and P. Lozano, J. Appl. Phys. 94, 3599 (2003)
[7] D. Garoz, *et al.,* J. Appl. Phys. 102, 094310 (2007)
[8] S. Castro *et al.*, J. Appl. Phys. 101, 084303 (2007)
[9] C. Larriba, S. Castro, J. Fernandez de la Mora, and P. Lozano, J. Appl. Phys. 101, 084303 (2007)
[10] R. S. Legge and P.C. Lozano, J. Propul. Power 27, 485 (2011)
[11] D. Courtney, H. Li, and P. Lozano, J. Phys. D: Appl. Phys. 45, 485203 (2012)
[12] R. Brandt, R. Petricevic, H. Probstle, and J. Fricke, J. Porous Mater. 10, 171 (2003)
[13] S. Mezzavilla, C. Zanella, P.R. Aravind, C. Della Volpe, and G.D. Soraru, J. Mater. Sci 47, 7175 (2012)
[14] M. Takeuchi, T. Hamaguchi, H. Ryuto, and G.H. Takaoka, Nucl. Instrum. Methods Phys. Res., Sect. B 315, 345 (2013)
[15] C.S. Perez-Martinez and P.C. Lozano, Appl. Phys. Lett. 107, 043501 (2015)
[16] R. Krpoun, K.L. Smith, J.P.W. Stark, and H.R. Shea, Appl. Phys. Lett. 94, 163502 (2009)
[17] C. Ryan, *et al.*, in AAAF-ESA-CNES Space Propulsion, Bordeaux, France (2012)
[18] D. Courtney and P. Lozano, "Ionic liquid ion source emitter arrays fabricated on bulk porous substrates or spacecraft propulsion", Ph.D. thesis (MIT, 2011)
[19] Z.-B. Zhou, H. Matsumoto, and K. Tatsumi, ChemPhysChem 6, 1324 (2005)
[20] T.F. Baumann, M.A. Worsley, T.Y.-J. Han and J.H. Satcher, J. Non-Cryst. Solids 354, 3513 (2008)
[21] S. Arestie, "Porous material and process development for electrospray propulsion applications," M.S. thesis (MIT, 2014)
[22] N. Brikner and P. Lozano, Appl. Phys. Lett. 101, 193504 (2012)
[23] N.A. Brikner, "On the identification and mitigation of life-limiting mechanisms of ionic liquid ion sources envisaged for propulsion of microspacecraft,", Ph.D. thesis (MIT, 2015)
[24] P. Lozano and M. Martinez-Sanchez, J. Phys. D: Appl. Phys. 38, 2371 (2005)
[25] P. Lozano, J. Phys. D: Appl. Phys. 39, 126 (2006)